J. Phys. Res. Edu., Vol. 1, March 2024

Variable thermoelectric parameters in Si / Ge zNR by electrostrictive application of localized strain

Amretashis Sengupta*

Department of Physics, P. D. Women's College, Jalpaiguri, West Bengal-735101, India

In this work, we propose the tuning of thermoelectric performance of zigzag monolayer Silicene and Germanene nanoribbon (SiNR/GeNR) with a reversible strain engineering method. By a proposed electrostrictive method a tensile or compressive moderate strain of ±2% orthogonal to the transport direction in a short region of the SiNR or GeNR is considered to be applied. A self-consistent density functional tight binding (DFTB) approach is employed for the calculation of the electronic properties of the system, while the vibrational properties are computed with classical molecular dynamics simulations. Electron/phonon transport is computed with the Green's function formalism. With the localized strain application it is observed that electron transmission and current through the Si or GeNR remains largely unaffected while a suppression of the phonon transport and thermal conductance can be achieved. A significant tuning is observed for thermoelectric figure of merit and variations are seen in the Seebeck coefficient and the thermoelectric power factor. Moreover the temperature and doping dependencies of these parameters also showed high degree of tunability with strain. The enhancements in thermoelectric figure of merit by such simple strain ON/OFF mechanism in a CMOS compatible architecture suggest good prospects for nanoscale thermoelectrics.

I. INTRODUCTION

Among the two-dimensional (2D) Dirac materials, Silicene and Germanene have general interest for the semiconductor industry due to their electronic properties and elemental familiarity with the planar CMOS process [1–8]. The prospect of these 2D materials for device and interconnect applications in the next generation of VLSI chips is realistic and also augers well for flexible electronics [5–8]. Moreover, such materials are also being explored for applications in optoelectronics, solar cells and chemical sensors [3–11].

Silicene and Germanene nanoribbons (SiNR and GeNR), have also been successfully synthesized [12] and studied in a number of theoretical and experimental works for their electrical parameters, spin transport, hydrogen sensing and other properties [2–16]. Like graphene nanoribbons these 1D nanostructures can be semi-metallic or metallic depending on their chirality and width [2–4, 17–19].

With the prospect of SiNR and GeNR interconnects and devices, the factor of application specific tai-

loring of material properties is also important. The electronic properties in Si and Ge 2D sheets are found to be altered with external electromagnetic or mechanical stimuli better than graphene due to their buckled honeycomb structure [3, 4, 20–22]. The tuning of electro-thermal properties in nanostructures made of Silicene or Germanene is also been investigated of late [20–30]. This is quite important from the point of view of thermoelectric devices, thermal management in integrated circuits and other applications such as NEMS. An important aspect of tailoring material properties in nanoelectronics application would be the reversibil-

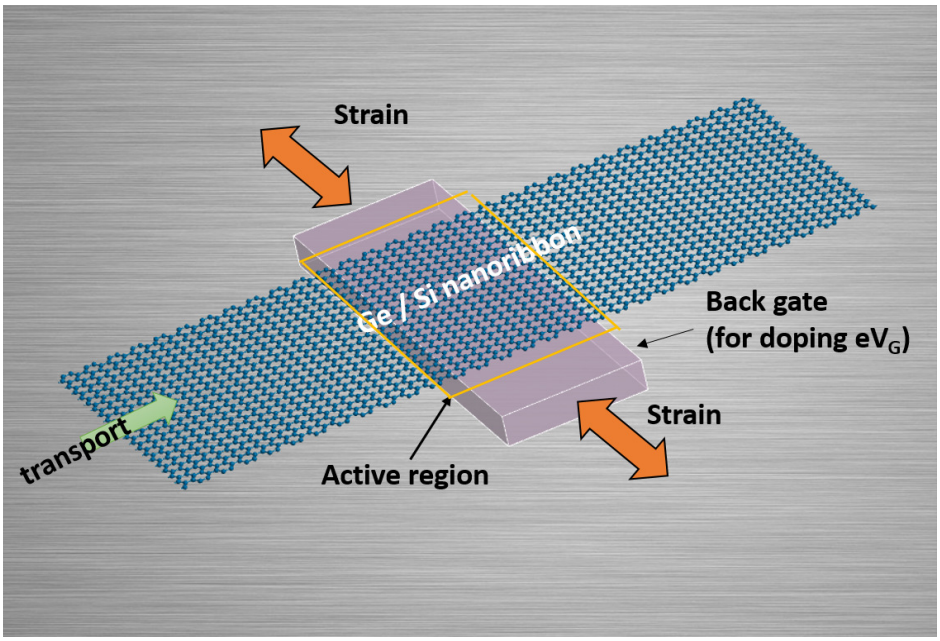

FIG. 1: Schematic of the proposed straining mechanism (not to scale).

ity of the induced enhancement/suppression of certain parameters. While much work has been carried out on the impact of line and point defects and dislocations on the thermoelectric behavior of Dirac materials [17–32] such topological changes are difficult to form in a controlled manner and are not something that can be switched on/off at will. The application of compressive vertical strain by means of electrostriction of a piezoelectric "gate" terminal to switch a bilayer MoS_2 channel has also been proposed by Das [33]. While this can be a highly efficient method to change electrical properties of multi-layered structures with changing the interlayer van der Waals gap, for monolayer systems the application of in-plane strain is more effective for tuning material properties [34] Such a system may be achieved by an in-plane electrostrictive architecture consisting of SiNR and GeNR being subject to a localized strain applied by a piezoelectric finger (or control bar) in a direction orthogonal to carrier transport [33, 34] Depending upon the polarity of the voltage applied on the bar the region of SiNR / GeNR suspended on it can be expanded and contracted. The issue of weak strain transfer in such an layered architecture may be mitigated by encapsulation

of the region of SiNR or GeNR within the piezo-material, such as ZnO or PMN-PT. This gives rise to three possible states of such a system/ device, the perfect state where no bias is applied to the control bar, the state of tensile (positive) strain, and that of compressive (negative) strain. Fig. 1 shows the schematic of the proposed straining mechanism.

Considering a moderate strain of ±2% and the perfect case (0% strain), we compute the electronic and thermo-electric parameters of zigzag SiNR and GeNR devices by means of atomistic simulations. With density functional tight binding (DFTB) formalism [35–37] the electronic properties of the system are evaluated, while the phonon calculations are performed with the frozen phonon approximation [38, 39] with a small-displacement method using classical potentials [38, 40, 41] The electron and phonon transport calculations are done with the Landuer approach within the non-equilibrium Green function (NEGF) framework [38, 42–46]. The thermoelectric parameters were evaluated with the PyQuanTE code [32] We calculate the carrier transport, phonon transmission, spectral currents and the various thermoelectric parameters namely the Peltier and Seebeck coefficients, thermoelectric conductance, thermoelectric figure of merit and the thermoelectric power factor. The variation of thermoelectric parameters with temperature was also studied in detail.

II. METHODOLOGY

We consider$(8, 8)$ zigzag SiNR and GeNR with comparable width of ∼5.5 nm. The proposed device consists of ideal semi-infinite contacts connected to a central region which is about 25 nm long. At the middle of this central region the ±2% strain is considered on a section of 5 nm long 'active' area (indicated in the schematic Fig. 1). The length of the central region ensures sufficient screening distance available on both sides of this active area, so as to properly match with the perfect contacts.

With density functional tight binding (DFTB) formalism the electronic properties of the system is simulated [38]. The tight binding method is chosen for it's high computational efficiency for handling systems with such large number of atoms. We use the Slater-Koster parameters for Si and Ge [38, 47] for our calculations. $1 \times 1 \times 24$ k-points in a Monkhorst-Pack grid [48] are used for sampling the device supercell. The phonon calculations are carried out under the frozen phonon approximation [38, 39] using the classical Stillinger-Weber [40, 41] type classical potential. A central finite difference method, inclusive of the acoustic sum rule with 180 atomic displacements of 0.01 magnitude, was employed for calculation of the symmetric dynamical matrix.

The electron current flowing between the two semi-infinite ideal contacts (1 and 2) is evaluated with

Landauer formula [42–45]

$$I = \frac{q}{h} \int_{-\infty}^{+\infty} dE \, \mathrm{Im}_{el}(E) \left[f_{FD}\left(E - \mu_1, T_1\right) - f_{FD}\left(E - \mu_2, T_2\right) \right], \tag{1}$$

where $f_{FD}(.)$ is the Fermi-Dirac distribution function, μ and T the electrochemical potential and the temperature of the contacts respectively, and Im_{el} the electron transmission function. For a small temperature difference, the electrical conductance derived from Eq. (1) has the following form [32, 38, 46]

$$G_e = \frac{2e^2}{h} \int_{-\infty}^{+\infty} dE \, \mathrm{Im}_{el}(E) \left(-\frac{df_{FD}(E,T)}{dE} \right). \tag{2}$$

The heat current I_Q develops between contacts due to temperature gradient and is related to the thermal conductance κ as [32–38]

$$\kappa = \left. \frac{dI_Q}{dT} \right|_{I=0}. \tag{3}$$

The methodology for electron transport and phonon transport is available in detail in standard literature, such as Refs. [42–46].

The electron thermal conductance can be written as [32]

$$\kappa_e = \frac{2}{k_B T^2 h} \left(L_2 - \frac{L_1^2}{L_0} \right), \tag{4}$$

where the Onsager coefficient L_n is expressed as [32, 49]

$$L_n = \int_{-\infty}^{+\infty} dE (E - E_F)^n \mathrm{Im}_{el}(E) \left(-\frac{df_{FD}(E,T)}{dE} \right). \tag{5}$$

In the low temperature difference limit, the phonon thermal conductance can be defined as

$$\kappa_{ph} = \int_{-\infty}^{+\infty} \frac{d\omega}{2\pi} \hbar\omega \, \mathrm{Im}_{ph}(\omega) \left(\frac{\partial f_{BE}(\omega,T)}{\partial T} \right), \tag{6}$$

where Im_{ph} is the phonon transmission, $f_{BE}(.)$ is the Bose-Einstein distribution function and ω the phonon frequency.

The Seebeck coefficient or thermopower (S) can be expressed as [45–49]

$$S(T) = -\frac{1}{eT} \frac{L_1}{L_0}. \tag{7}$$

The thermoelectric figure of merit ZT is given as [45–49]

$$ZT = \frac{G_e S^2 T}{\kappa_e + \kappa_{ph}}. \tag{8}$$

III. RESULTS AND DISCUSSION

In our calculations the electron-phonon and the phonon-phonon couplings were not taken into account since the scattering length in such Dirac materials greatly exceed the dimensions considered herein [2, 3, 17–32].

The phonon transmission spectra as in Fig. 2(b) shows significant suppression upon the application of ±2% strain in the NR structures. A tensile strain shows slightly less suppression at lower energies as compared to compressive strain for GeNR. For the SiNR both strained conditions show a very similar nature of reduction from the unstrained condition. For GeNR the phonon transmission states exist mostly between 0 to 0.04 eV, for SiNR the range expands to 0 to 0.08 eV. The greater suppression of the phonon transmission against electron transmission upon introduction of non-uniformity in lattice is something that is observed in other 1 dimensional systems as CNTs [32].

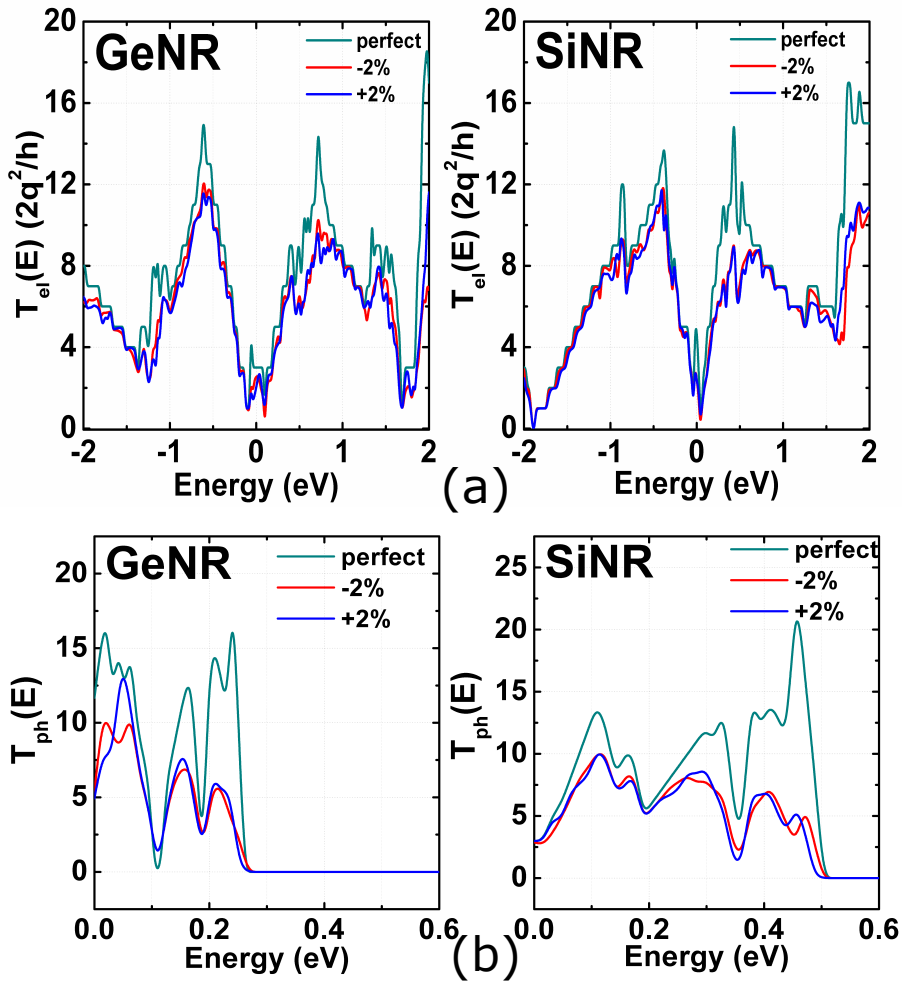

FIG. 2: (a) Electron and (b) phonon transmission spectra of the various devices at equilibrium condition.

In Fig. 3, the conductance of the various conditions of the SiNR and GeNR systems for variation in temperature and Fermi level position is shown. The change in fermi level position is considered resulting from a variation in chemical doping or electrostatic doping by the application of a gate voltage (VG). We designate this Fermi level modulation as eV_G in our plots and refer to them as simply doping. We see that with the increase in temperature the peaks of the conductance reduces in magnitude, at the same time the peaks become more broadened and less strong for the same amount of doping.

In the presence of a symmetry breaking event as strain, the coherence of the transmission states is lost to some degree resulting in the reduction in the conductance. The distinct fluctuations at 100 K smoothen out as the temperature is increased and can be attributed to change in the Fermi distribution of the system. The conductance in both SiNR and GeNR seem vary more with change in temperature, near the maxima or minima than in other positions of the plots. Also the GeNR displays slightly more conductance against SiNR structures for higher amounts of doping.

Coming to the thermal conductivities in Fig. 4, we can see a reduction in the thermal conductivity of the SiNR and GeNR configurations upon the application of both tensile and compressive localized strain. This is consistent with our aim of enhancing thermoelectric qualities of the nanoribbons with strain engineering. For the low temperatures the contribution due to phonons is shown by dashed lines. An interesting observation at this point is the dominance of the electron contribution to the thermal conductivity over the lattice part which is largely due to the metallic nature of zigzag SiNR and GeNR. For these NRs the electronic κ_e and lattice κ_{ph} part of the thermal conductivity are at best equal at low doping levels at 100 K while for 300 K and above the electronic part becomes dominant even for the undoped condition.

The Seebeck coefficients of the SiNR and GeNR shown in Fig. 5, show a minor increase with strain application (both tensile and compressive) for the same level of doping at temperatures in excess of 300 K. In the SiNR it is seen that with increase in negative doping and temperature the plots tend to bunch together more than that in case of GeNR. An oscillatory behavior of S with doping is seen in all cases, with a gradual smoothing of the fluctuations with increase in temperature. Even at temperatures at and above 300 K, the change of sign of the Seebeck coefficient with change in doping sign and also magnitude is present. For instance, for the GeNR a changeover from positive values to negative value of Seebeck coefficient occurs around -0.6 eV for the GeNR. On the positive doping side a changeover of S from the negative to positive value occurs around 0.8 eV for the GeNR. For SiNR these turning point is around -0.4 eV ($S > 0$ to $S < 0$) and +0.4 eV (for $S < 0$ to $S > 0$). This indicates a modulation of the thermal transport behavior between electron dominated (where $S < 0$) and hole dominated (where $S > 0$) regimes in such SiNR and GeNR systems as the doping and temperature changes.

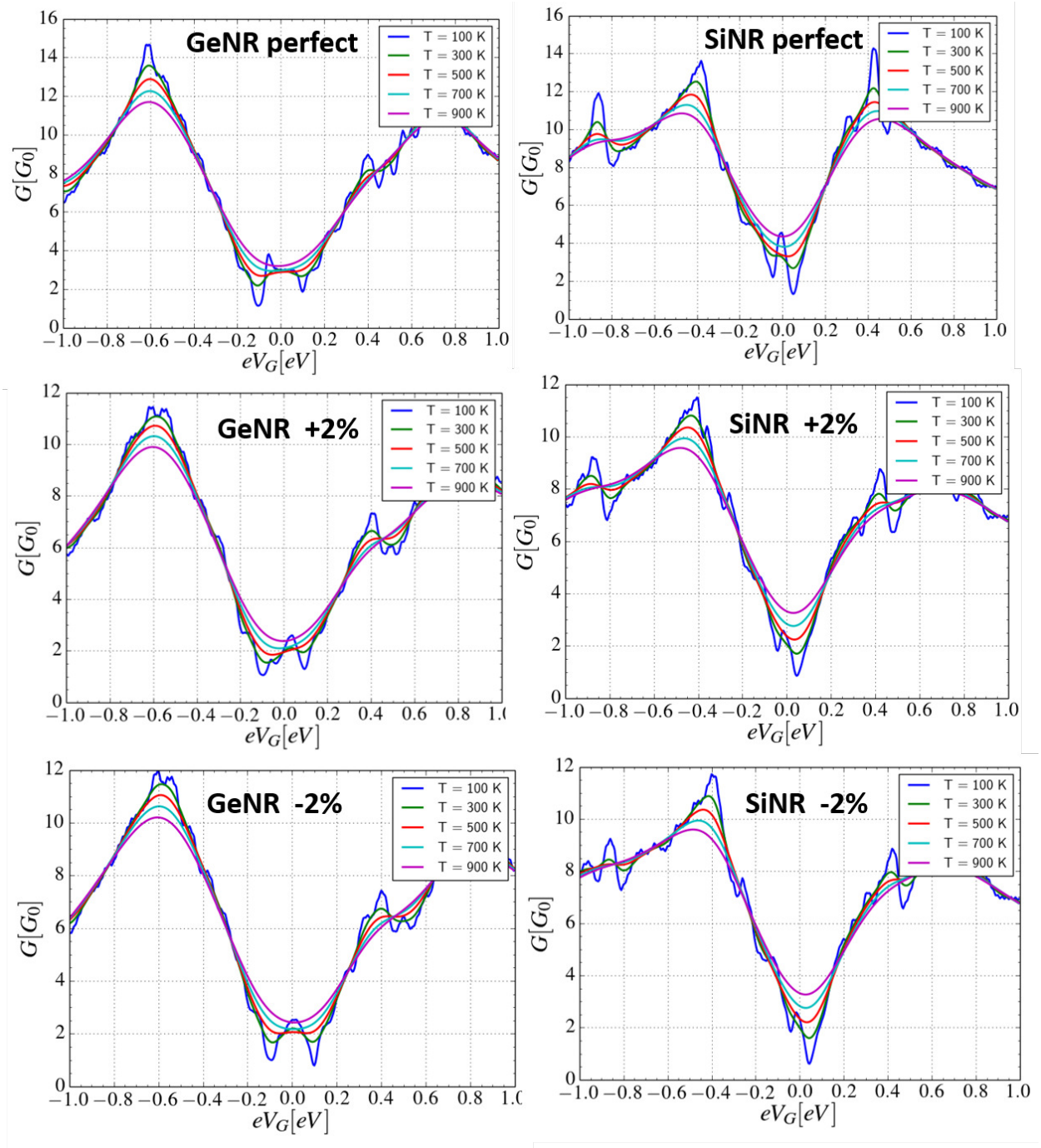

FIG. 3: Variation of conductance (G) of the SiNR and GeNR for different conditions with doping and temperature.

The thermoelectric figure of merit (ZT) plotted in Fig. 6, shows more diverse behavior in terms of change of material and strain than other thermoelectric coefficients presented earlier. The peak values of the figure of merit differ depending on the material, temperature and nature of strain and are usually between 0.12-0.25, which is acceptable considering the single layered one dimensional structures considered in our

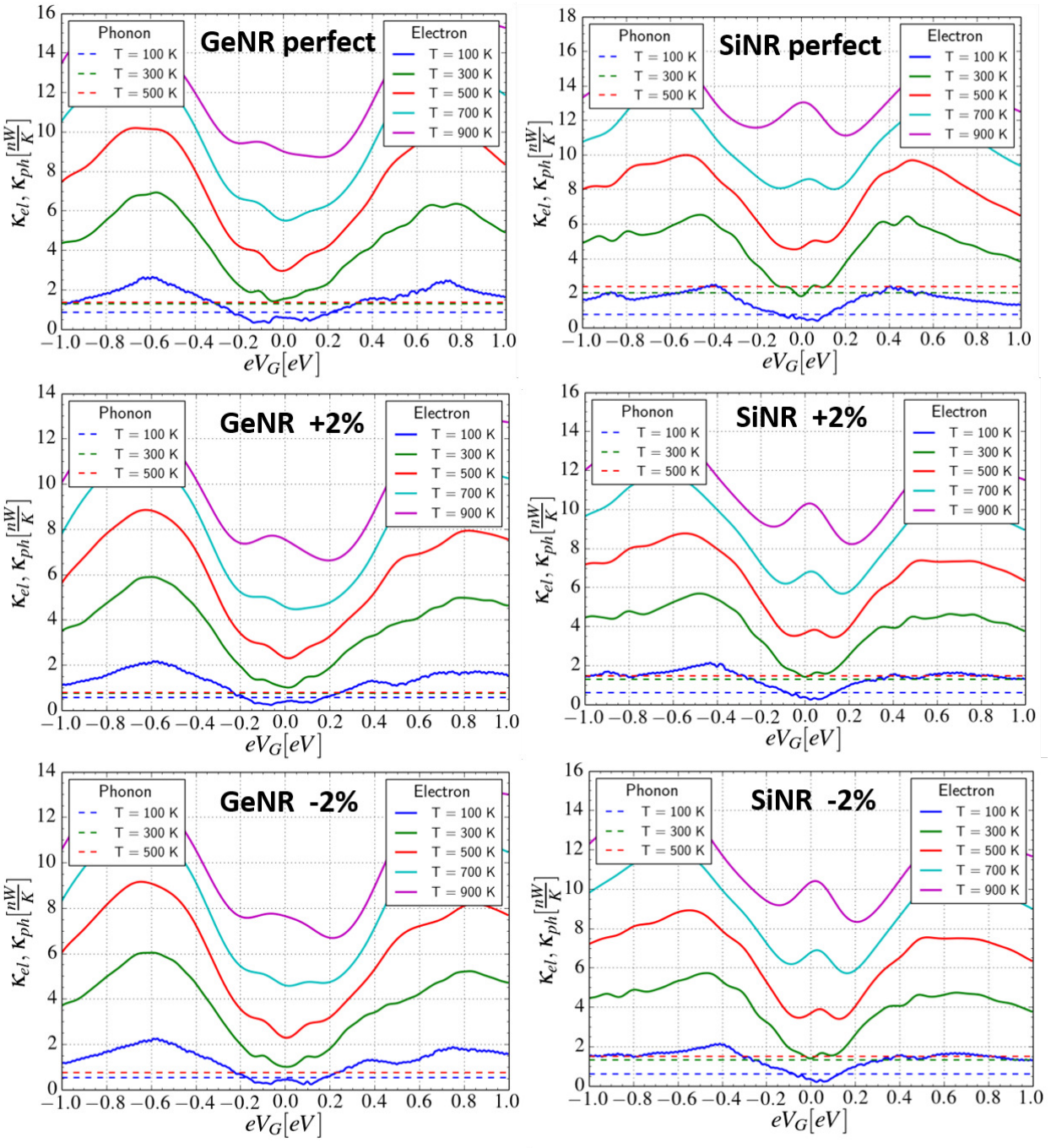

FIG. 4: Variation of thermal conductance ($\kappa_{e,ph}$) of the SiNR and GeNR for different conditions with doping and temperature. Electronic part shown in solid lines, while lattice (phonon) part shown in dotted lines.

studies. It is seen in SiNR that at very low doping levels and low temperature of 100 K, ZT shows values larger than that for temperatures of 300 K and above for similar doping. For SiNR with increase in temperature the ZT plot spreads out more and has a lesser maxima at the same positive doping value, which

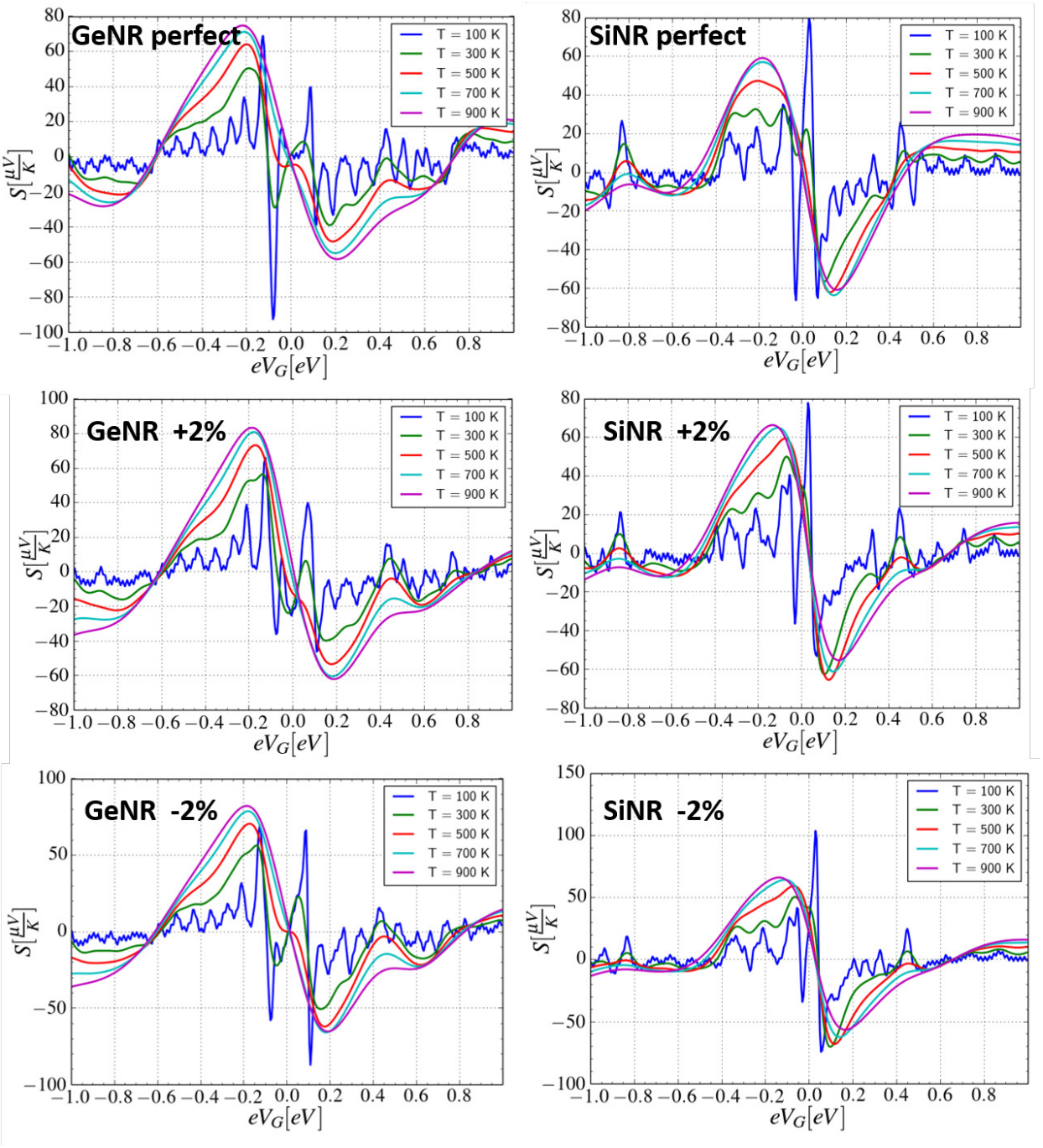

FIG. 5: Variation of Seebeck coefficient (S) of the SiNR and GeNR for different conditions with doping and temperature.

is different from GeNR. With application of strain, the most significant increase in ZT is seen in SiNR, where for temperatures of 300 K and above a $\sim$30-35% increase is seen ZT for minor doping levels with $\pm$2% localized strain. Also this enhancement in SiNR is more for the negative doping than positive doping values. In GeNR at temperatures above 300 K a higher degree of ZT enhancement of about 25% can be

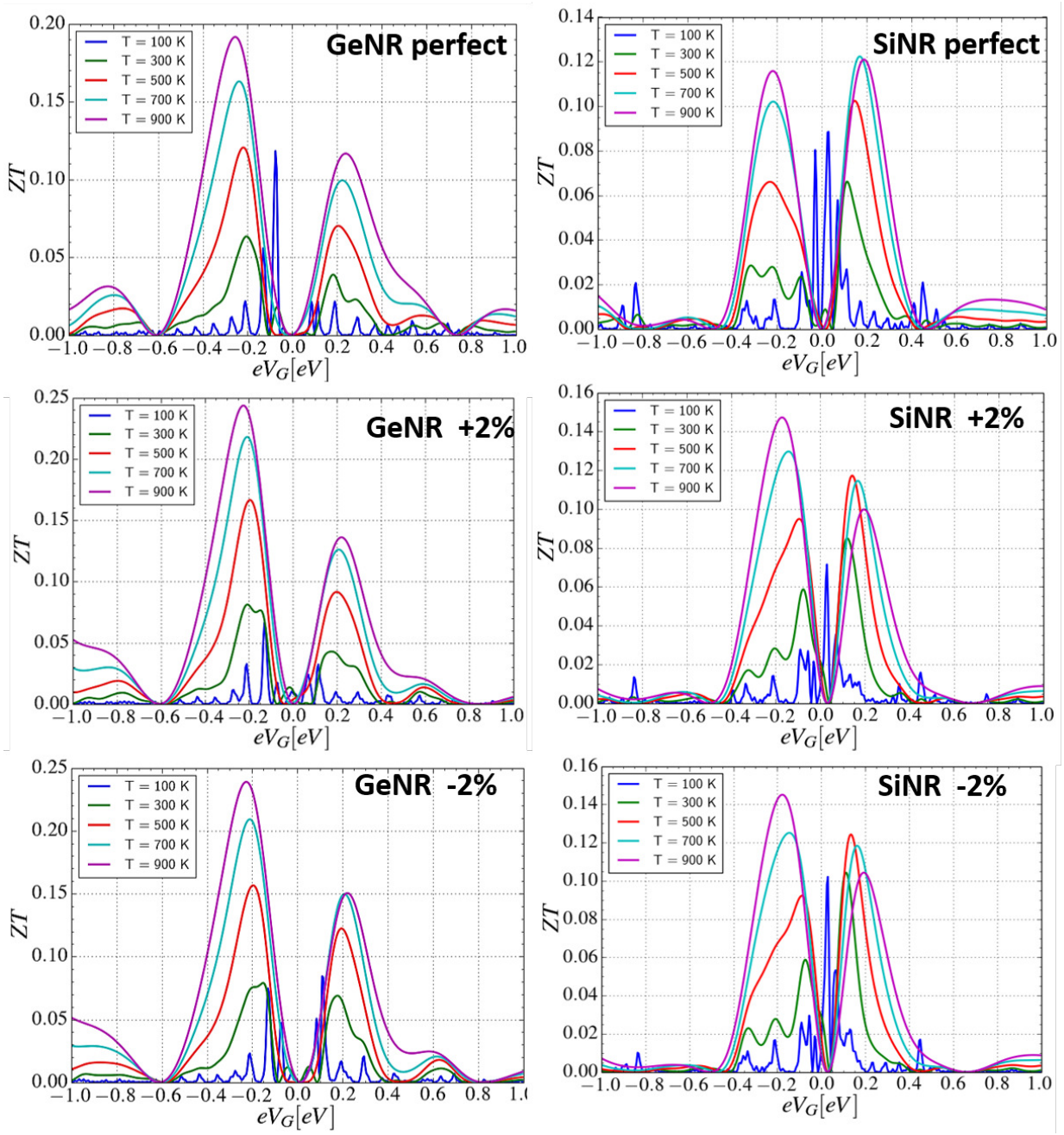

FIG. 6: Variation of the thermoelectric figure of merit (ZT) of the SiNR and GeNR for different conditions with doping and temperature.

seen for $\pm 2\%$ of strain. These results indicate that by applying a moderate strain($\pm 2\%$) on a small section of a 1D SiNR or GeNR, it is possible to significantly tune the thermoelectric behavior of the material up to 35% for SiNR 25% for GeNR. The reversible nature of the induced deformation, makes it a good candidate for tunable thermoelectric devices/ interconnects.

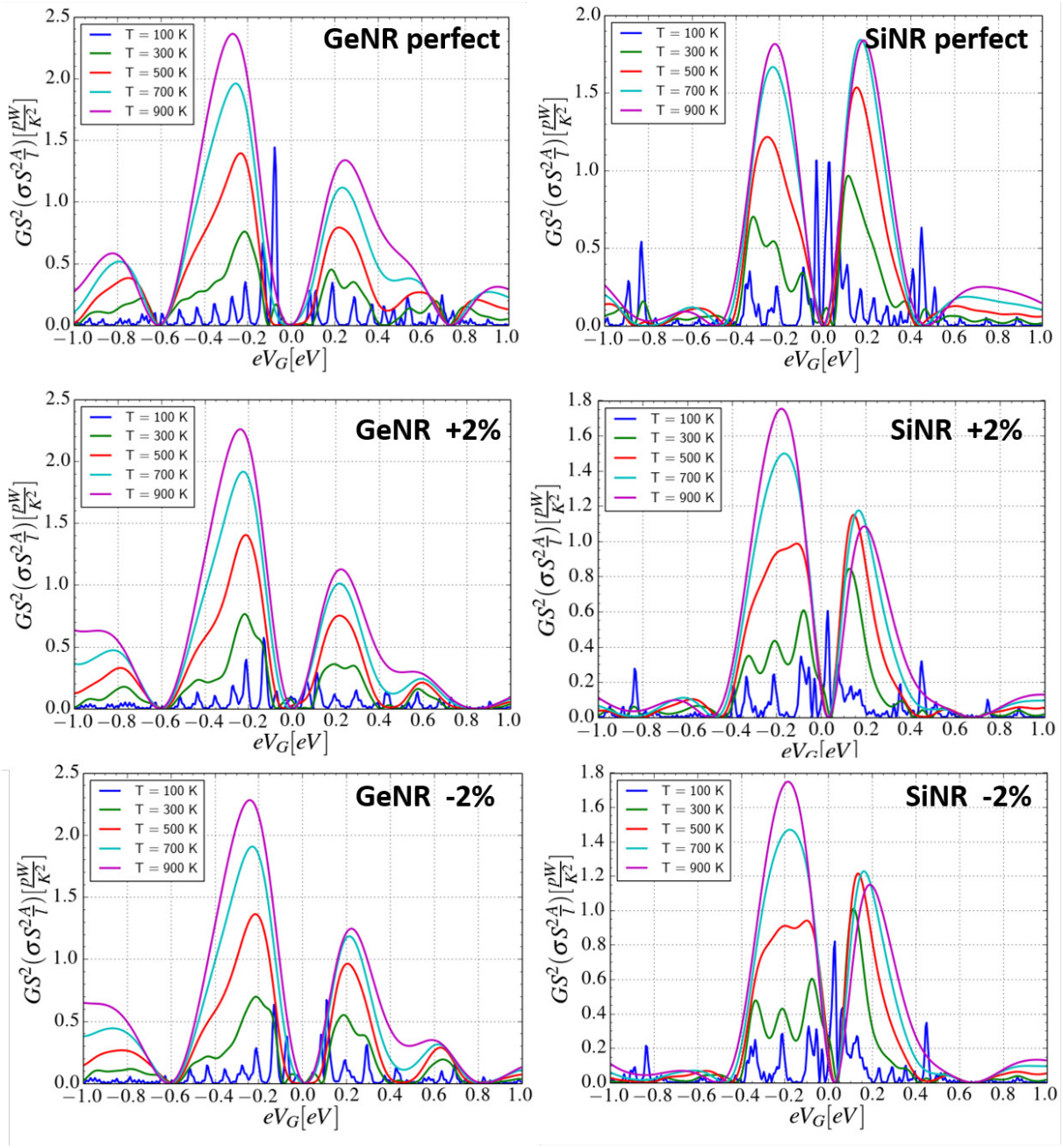

FIG. 7: Variation of the thermoelectric power factor of the SiNR and GeNR for different conditions with doping and temperature.

The thermoelectric power factor(PF), shown in Fig. 7, also confirms tuning with application of strain. The response however is a different for SiNR and GeNR structures. Overall there is a rather minor change in case of the PF for the GeNR with negative doping and a slight decrease in the maxima of the power factor, for the positive doping. The SiNR however shows a marked increase in PF with $\pm 2\%$ strain for the low negative doping region, especially at 300 K. For doping levels of -0.2 eV, the PF rises about 3-4 times

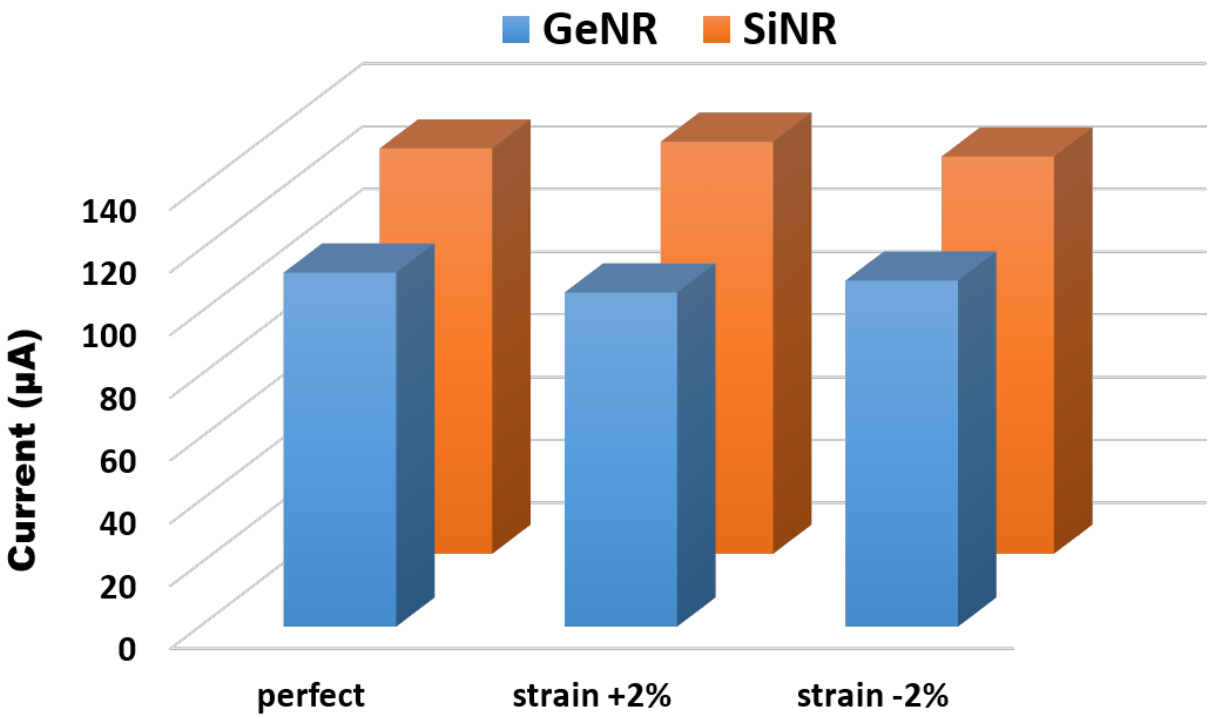

FIG. 8: Variation of the current through the SiNR and GeNR structures at a driving voltage of 1V.

for 300 K operating temperature.

While engineering the thermoelectric properties it is important to reduce thermal conductivity while ensuring minimal effect on the electrical conduction. In order to investigate the effects of strain on the electrical current in the SiNR and GeNR, we carried out non-equilibrium Green function (NEGF) simulations for a moderate bias of 1 V (at 300 K) and evaluated the maximum ballistic current with the two probe Landauer method. The results (Fig. 8) show that the zigzag SiNR and GeNR structures can offer a good driving current in the range of 90-120 μA and the effect of localized strain on the output current is rather small($< 5 - 7\%$). This is quite a positive factor considering the aim in thermoelectric tuning is to have variation in the heat transport properties of a system without much significantly affecting the electronic transport. Since Silicene or Germanene are Dirac materials, through charge pumping or adsorption doping they can be rather easily modulated between n-type or p-type materials [50]. Reports regarding silicene based TEGs have also appeared [51].

IV. CONCLUSION

In this work we explore how a reversible effect as in-plane strain application in a localized manner can be employed to tune the thermoelectric properties of zigzag silicene and germanene nanoribbons. With atomistic simulations we investigate the electron transmission properties and with classical potentials the phonon properties are investigated. The thermoelectric properties are evaluated from the electron and the phonon transmission spectrum calculated under the NEGF formalism. Our studies show a good degree of tuning of electrothermal coefficients are attainable by such strain engineering in SiNR and GeNR systems. A suppression of thermal conductivity while keeping the electronic transport not as much affected was possible to achieve in particular for both the SiNR and the GeNR systems. For GeNR and SiNR devices, 25% and 35%, respectively enhancement is seen in ZT for similar conditions by application of the moderate strain of ±2% in a small portion of the entire NR. These results indicate a good prospect of controlling the electrothermal performance of SiNR and GeNR structures with a simple mechanism and is important from the point of view of nanoscale thermoelectrics in next generation devices and sensors.

ACKNOWLEDGEMENTS

A. S. thanks SERB, India for the SERB Research Scientist Fellowship. A.S. also wishes to thank Dr. Dmitry A. Ryndyk of BCCMS, University of Bremen for valuable comments and discussions.

* Electronic address: amretashis@gmail.com

[1] A. Molle, J. Goldberger, M. Houssa, Y. Xu, S.-C. Zhang, and D. Akinwande, Nat. Mater. **16**, 163 (2017).

[2] J. Zhao, H. Liu, Z. Yu, R. Quhe, S. Zhou, Y. Wang, C.C. Liu, H. Zhong, N. Han, J. Lu, Y. Yao, and K. Wu, Prog. Mater. Sci. **83**, 24 (2016).

[3] A. Acun, L. Zhang, P. Bampoulis, M. Farmanbar, A. van Houselt, A.N. Rudenko, M. Lingenfelder, G. Brocks, B. Poelsema, M.I. Katsnelson, and H.J.W. Zandvliet, J. Phys. Condens. Matter **27**, 443002 (2015).

[4] M.E. Davila and G. Le Lay, Sci. Rep. **6**, 20714 (2016).

[5] L. Tao, E. Cinquanta, D. Chiappe, C. Grazianetti, M. Fanciulli, M. Dubey, A. Molle, and D. Akinwande, Nat. Nanotechnol. **10**, 227 (2015).

[6] G. Fiori, F. Bonaccorso, G. Iannaccone, T. Palacios, D. Neumaier, A. Seabaugh, S.K. Banerjee, and L. Colombo, Nat. Nanotechnol. **9**, 768 (2014).

[7] S. Yamacli, J. Nanoparticle Res. **16**, 2576 (2014).

[8] A.H. Bayani, D. Dideban, and N. Moezi, J. Comput. Electron. **15**, 381 (2016).

[9] A.H. Bayani, D. Dideban, M. Vali, and N. Moezi, Semicond. Sci. Technol. **31**, 045009 (2016).

[10] Y. Wang, Z. Ni, Q. Liu, R. Quhe, J. Zheng, and M. Ye. Adv. Funct Mater. **25**, 68 (2015).

[11] S. Wippermann, Y. He, M. Voros, and G. Galli, Appl. Phys. Rev. **3**, 040807 (2016).

[12] M.R. Tchalala, H. Enriquez, A.J. Mayne, A. Kara, G. Dujardin, M.A. Ali, and H. Oughaddou, J. Phys. Conf. Ser. **491**, 12002 (2014).

[13] B. Aufray, A. Kara, S. Vizzini, H. Oughaddou, C. Ĺandri, B. Ealet, and G. Le Lay, Appl. Phys. Lett. **96**, 183102 (2010).

[14] M. Derivaz, D. Dentel, R. Stephan, M.C. Hanf, A. Mehdaoui, P. Sonnet, and C. Pirri, Nano Lett. **15**, 2510 (2015).

[15] P. De Padova, O. Kubo, B. Olivieri, C. Quaresima, T. Nakayama, M. Aono, and G. Le Lay, Nano Lett. **12**, 5500 (2012).

[16] P. De Padova, C. Quaresima, C. Ottaviani, P.M. Sheverdyaeva, P. Moras, C. Carbone, D. Topwal, B. Olivieri, A. Kara, H. Oughaddou, B. Aufray, and G. Le Lay, Appl. Phys. Lett. **96**, 261905 (2010).

[17] M. Houssa, A. Dimoulas, and A. Molle, J. Phys. Condens. Matter **27**, 253002 (2015).

[18] B. Zhou, B. Zhou, Y. Zeng, G. Zhou, and M. Duan, Phys. Lett. A **380**, 282 (2016).

[19] Q. Pang, Y. Zhang, J.-M. Zhang, V. Ji, and K.-W. Xu, Nanoscale **3**, 4330 (2011).

[20] S. Mehdi Aghaei and I. Calizo, J. Appl. Phys. **118**, 104304 (2015).

[21] L. Matthes and F. Bechstedt, Phys. Rev. B **90**, 165431 (2014).

[22] Z. Ni, Q. Liu, K. Tang, J. Zheng, J. Zhou, R. Qin, Z. Gao, D. Yu, and J. Lu, Nano Lett. **12**, 113 (2012).

[23] W. Zhao, Z.X. Guo, Y. Zhang, J.W. Ding, and X.J. Zheng, Solid State Commun. **227**, 1 (2016).

[24] H. Sadeghi, S. Sangtarash, and C.J. Lambert, Sci. Rep. 5, 9514 (2015).

[25] K. Zberecki, M. Wierzbicki, J. Barnaa, and R. Swirkowicz, Phys. Rev. B **88**, 115404 (2013).

[26] K. Yang, S. Cahangirov, A. Cantarero, A. Rubio, and R. D'Agosta, Phys. Rev. B **89**, 125403 (2014).

[27] L. Pan, H.J. Liu, X.J. Tan, H.Y. Lv, J. Shi, X.F. Tang, and G. Zheng, Phys. Chem. Chem. Phys. **14**, 13588 (2012).

[28] M. Hu, X. Zhang, and D. Poulikakos, Phys. Rev. B. **87**, 195417 (2013).

[29] S.M. Aghaei and I. Calizo, Conf. Proc. - IEEE SOUTHEASTCON 2015–June, (2015).

[30] A. Sengupta, Proc. SISPAD 2016, pp. 97-100 (2016).

[31] D. Saha, A. Sengupta, S. Bhattacharya, and S. Mahapatra, J. Comput. Electron. **13**, 862 (2014).

[32] T. Lehmann, D.A. Ryndyk, and G. Cuniberti, Phys. Status Solidi Appl. Mater. Sci. **213**, 591 (2016).

[33] S. Das, Sci. Rep. **6**, 34811 (2016).

[34] R. Roldan, A. Castellanos-Gomez, E. Cappelluti and F. Guinea, J. Physics. Condens. Matter **27**, 313201 (2015).

[35] D. Porezag, T. Frauenheim, T. Köhler, G. Seifert, and R. Kaschner, Phys. Rev. B **51**, 12947 (1995).

[36] G. Seifert, D. Porezag, and T. Frauenheim, Int. J. Quantum Chemistry **58**, 185 (1996).

[37] A. Pecchia and A. Di Carlo, Rep. Prog. Phys. **67**, 1497 (2004).

[38] DFTB+ code available online www.dftb.org.

[39] K. Kaasbjerg, K.S. Thygesen, and K.W. Jacobsen, Phys. Rev. B **85**, 115317 (2012).

[40] F.H. Stillinger and T. A. Weber, Phys. Rev. B, **31**, 5262 (1985).

[41] https://www.tremolo-x.com/.

[42] G. Jha and T. Heine, J. Chem. Theory Comput. **18**, 7, 4472 (2022).

[43] J. Guo, M. Lundstrom, and S. Datta, Appl. Phys. Lett. **80**, 3192 (2002).

[44] S. Datta, Quantum Transport: Atom to Transistor, (Cambridge University Press, NY 2005).

[45] J. Guo, S. Datta, M. Lundstrom, and M. P. Anantram, Int. J. Multiscale Computational Engineering **2**, 257 (2004).

[46] D.A. Ryndyk, Theory of quantum transport at nanoscale, (Springer, Heidelberg, 2016).

[47] P. Vogl, H.P. Hjalmarson, and J.D. Dow, J. Phys. Chem. Solids **44**, 365 (1983).

[48] H. J. Monkhorst, and J. D. Pack, Phys. Rev. B **13**, 5188 (1976).

[49] T. Markussen, A.-P. Jauho , and M. Brandbyge, Phys. Rev. Lett. **103**, 055502 (2009).

[50] Z. Ni *et al*, Nanoscale **6**, 7609 (2014).

[51] M. M. El Banna, A.H. Phillips, A.S. Bayemi, IEEE Access, **9**, 103564 (2021).